Use of l-dependent pseudopotentials in the study of alkali-metal-atom—He systems. The adiabatic molecular potentials

J. Pascale
Service de Physique des Atomes et des Surfaces, Centre d'Etudes Nucléaires de Saclay, F-91191 Gif-sur-Yvette Cedex, France
(Received 15 February 1983)

Molecular-structure calculations have been performed to obtain the adiabatic potentials for ground state and numerous excited states of alkali-metal—He systems. They use l-dependent pseudopotentials defined from spectroscopy data or scattering data to describe the e^--M^+ and e^--He interactions (where M is any alkali-metal atom). Standard variational calculations are made, and a large basis set of Slater-type orbitals is used in order to ensure accuracy and stability of the results. Our results are discussed along with comparisons with other theoretical and experimental data. The overall agreement which has been obtained with all available experimental data indicates that significant improvements in the calculation of the M-He adiabatic potentials have been achieved by using an l-dependent pseudopotential technique.

I. INTRODUCTION

Much experimental and theoretical work[1] has been devoted in recent years to the study of various processes occurring in thermal collisions between ground-state or excited alkali-metal atoms and ground-state rare-gas atoms, such as alkali-metal intradoublet or interdoublet transitions, quenching of alkali-metal excited levels, alkali-metal pressure spectral line broadening, etc. Because the interatomic interactions are the main physical quantities needed for a good understanding of these collisional processes, much effort has been devoted to calculating[2–12] or experimentally determining[13–18] the adiabatic potentials of the alkali-metal—rare-gas systems. Standard *ab initio* calculations of the adiabatic potentials,[3,4] which can, in principle, be very accurate when enough electronic configurations are included in the calculations, become rapidly difficult and costly to perform as the number of electrons in the atomic cores increases. Calculations using model potentials or pseudopotentials offer a very interesting alternative to treat the problem.[5–12,19] They take advantage of the fact that the alkali-metal core and the rare-gas atom have closed-shell structures to reduce the problem of the alkali-metal—rare-gas interaction to a three-body problem (alkali-metal core, valence electron, and rare-gas atom). In both techniques, an effective potential is defined to represent the potential experienced by the valence electron. It simulates incomplete screening of the nuclear charge due to the core electrons, and it can also include the polarization interactions. In the pseudopotential technique, the effective potential also simulates the antisymmetry effects due to the Pauli principle by a repulsive potential; therefore it is l dependent and the lowest radial wave function is nodeless for an l series. In the model potential technique, the valence-electron wave function must be orthogonal to all the orbitals of the core and must have the correct number of nodes. These techniques, when correctly applied, can give reliable results,[7–9,12,10] in particular, outside the region where the two atomic cores overlap. The pseudopotential technique appears, however, to be the most convenient for molecular-structure calculations because the core orbitals do not have to be included in the atomic basis-set expansion of the molecular wave function.

Extensive pseudopotential molecular-structure calculations for all the alkali-metal—rare-gas systems were made[2,6] using an l-independent Gombàs-type statistical pseudopotential to represent the interaction between the alkali-metal valence electron and the rare-gas atom. These results have been very useful to semiquantitatively interpret, or predict various collisional processes, for example, the alkali-metal $n\,^2P$ fine-structure transitions which may result predominantly from a nonadiabatic coupling at intermediate internuclear distances ($\sim$10—14 a.u.), a region where these calculations were expected to be relatively accurate. However, with a growing amount of accurate experimental data, it has became necessary to improve such calculations, in particular, for the lightest rare-gas atoms for which both the use of a statistical pseudopotential and the non-l-dependence of the potential were questionable. Some attempts to improve these calculations have been made recently,[10,11] but again used an l-independent pseudopotential and therefore were proving completely unsuccessful in the cases of He and Ne.

We have undertaken extensive and accurate l-dependent pseudopotential calculations for alkali-metal—rare-gas systems, beginning with M-He systems. A few results have already been reported for NaHe and CsHe systems,[21] indicating a large improvement over all previous calculations. The method that we have adopted to calculate the adiabatic potentials is different to that used previously.[6] In fact, the use of an l-dependent statistical pseudopotential as suggested by Gombàs to represent the e^-—rare-gas-atom interaction seems to be cumbersome and, moreover, cannot reproduce correctly all the experimental phase shifts of the e^-—rare-gas-atom scattering. Therefore we thought it preferable to define the l-dependent pseudopotentials which represent the e^--M^+ or e^-—rare-gas-atom interactions from experimental data and to calculate the adiabatic potentials from standard variational calculations using Slater-type orbitals (STO). In this paper we discuss the method of calculation and present detailed results on the adiabatic potentials of ground state and numerous ex-

cited states of all the M-He systems. Our results are discussed in relation to available experimental data and theoretical results.

II. METHOD OF CALCULATION

A. Generalities

The use of pseudopotentials in molecular-structure calculations is fairly well established.[19] We briefly recall the method and discuss the way in which we determine the interactions included in the Hamiltonian.

In the Born and Oppenheimer approximation, the calculation of the adiabatic potentials $E_i(R)$ for an alkali-metal—rare-gas system reduces to finding a solution for the one-electron Schrödinger equation at any given internuclear distance R:

$$[-\tfrac{1}{2}\nabla^2_{\vec{r}_A}+V_A(\vec{r}_A)+V_B(\vec{r}_B)+V_{CT}(\vec{r}_B,\vec{r}) +V_{AB}(\vec{R})-E_i(R)]\psi_i(\vec{r}_A,R)=0 , \quad (1)$$

where $\vec{r}_X$, $X\equiv A,B$ is the position vector of the alkali-metal valence electron e^- with respect to the alkali-metal core (A) or the rare-gas atom (B), and $\vec{R}$ is the position vector of B with respect to A. $V_X(\vec{r}_X)$ is an effective potential describing the interaction between e^- and the core X, which is modeled, depending on the core X, from spectroscopic or scattering experimental data; it contains a long-range part including polarization terms, and an l-dependent pseudopotential describing the short-range interaction. $V_{CT}(\vec{r}_B,\vec{R})$ is the well-known cross term or three-body interaction[2,12] which arises from the polarization of B by both e^- and A. Finally, $V_{AB}(R)$ is a potential depending only on R, which estimates the interaction between A^+ and B. The spin-orbit interaction is not included in the present calculations.

Equation (1) is solved using a standard variations procedure from an expansion of the molecular wave function $\psi_i(\vec{r}_A,R)$ over a STO basis set centered on the alkali-metal core.

B. Effective potential $V_X(\vec{r}_X)$

The interaction between e^- and X is represented by

$$V_X(\vec{r}_X)=V_X^{sr}(\vec{r}_X)-\frac{Z_X}{r_X}-\frac{1}{2}\frac{\alpha_{dX}}{(r_X^2+d_X^2)^2} -\frac{1}{2}\frac{\alpha'_{qX}}{(r_X^2+d_X^2)^3} , \quad (2)$$

where Z_X is the net charge of the core seen by e^- at an infinite distance, α_{dX} is the static dipole polarizability of X, and α'_{qX} is an effective quadrupole polarizability of X that we define as

$$\alpha'_{qX}=\alpha_{qX}-6\beta_X+2\alpha_{dX}d_X^2 . \quad (3)$$

The definition of α'_{qX} takes the dynamical correction $-6\beta_X$ to the static quadrupole polarizability α_{qX} into account; it also includes a term which balances the contribution of the dipole polarization term at large-r_X values resulting from our choice of cutoff function.

The cutoff function, with a cutoff radius d_X, is used to avoid any divergence of the polarization terms at $r_X=0$. The present choice, like any other one that might be made, is more or less arbitrary. In principle, however, it should not significantly affect the values of the calculated adiabatic potentials.[7]

$V_X^{sr}(\vec{r}_X)$ is an l-dependent short-range pseudopotential

$$V_X^{sr}(\vec{r}_X)=\sum_{l=0}^{\infty}\sum_{m=-l}^{+l} V_{Xl}^{sr}(r_X)\,|\,Y_{lm}(\hat{r}_X)\rangle\langle\,Y_{lm}(\hat{r}_X)\,| , \quad (4)$$

where $|\,Y_{lm}(\hat{r}_X)\rangle$ is a spherical-harmonic function centered on the core X ($\hat{r}_X=\vec{r}_X/r_X$); $V_{Xl}^{sr}(r_X)$ is chosen to be a Gaussian-type radial potential[19]

$$V_{Xl}^{sr}(r_X)=C_{Xl}\exp(-D_{Xl}r_X^2) , \quad (5)$$

where C_{Xl} and D_{Xl} are parameters. The role of the present pseudopotential is twofold. Firstly, it is to simulate by a repulsion the effects of the Pauli principle when the valence electron with l symmetry approaches X and there are some l electrons in the core. Secondly, it is to take into account incomplete screening of the nuclear charge due to the core electrons when e^- approaches the core, so that $V_{Xl}^{sr}(r_X)$ is attractive when there is no l electron in the core. Other analytical forms for $V_{Xl}^{sr}(r_X)$ could be chosen. The present form, with only two parameters, was found flexible enough, when associated with the correct long-range part of the effective potential, to represent the net

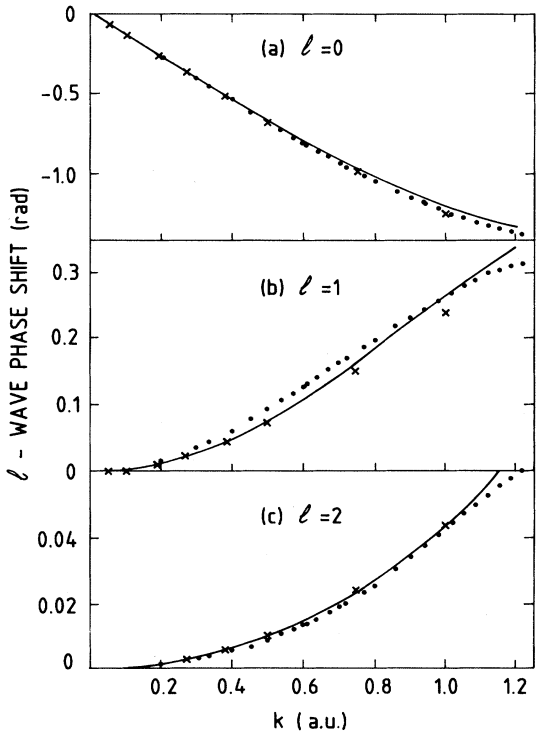

FIG. 1. l-wave phase shifts for e^--He elastic scattering vs wave number k: (a) s-wave phase shift (modulo II), (b) p wave, (c) d wave. Note the different vertical scales. ——, present results; ×, theoretical results of Valiron *et al.* (Ref. 20) (see Table I of the reference, potential $V1$); ●, experimental values of Williams (Ref. 25).

interaction experienced by e^- in the presence of an alkali-metal core or the He atom. In particular, a form using more than two parameters seems unnecessary and not suitable for molecular-structure calculations. In practice, the summation over l in Eq. (4) is limited to only a few values since e^- will experience the same radial potential, in addition to the centrifugal one, for l greater or equal to some value $l_{\max}$. In the case of He, $l_{\max}=1$.

For an alkali-metal ion, the parameters of the effective potential [see Eqs. (2) and (5)] were determined so as to reproduce the experimental ionization energies of the alkali-metal atom nl levels. For the present calculations we used the parameters $Z_A=1$, α_{dA}, α'_{qA}, d_A, C_{Al}, and D_{Al} reported in Table 13 of Ref. 19. They reproduce the experimental ionization energies of the nl levels to better than about 10^{-5} a.u. [atomic units are used unless otherwise specified] when the radial Schrödinger equation is directly integrated; when it is solved using a variational procedure, as was done to determine the nonlinear parameters of the STO in order to perform molecular-structure calculations, the ionization energies are generally reproduced with an accuracy better than 2.5×10^{-4} a.u., depending on the alkali-metal core and the l series involved.

For the He atom, $Z_B=0$, we took $\alpha_{dB}=1.3834$,[22] $\alpha_{qB}=2.3265$,[23] and $\beta_B=0.706$.[24] The other parameters involved in the expression for the effective potential were determined by fitting recent experimental l-wave phase shifts[25] ($l=0,1,2$) for e^--He elastic scattering, in the 0.58–20.0-eV energy range, together with a scattering length value of 1.177 (Ref. 26) considered to be the best available. It should be noted that, for the s wave, the experimental phase shifts were fitted modulo II as we used a pseudopotential. We obtained $d_B=1.0$, $C_{B\,l=0}=2.03$, $D_{B\,l=0}=0.463$, $C_{B\,l\geq1}=-1$, and $D_{B\,l\geq1}=1.0$. Our calculated phase shifts are shown in Fig. 1 along with the experimental data of Williams.[25] The experimental errors are about 1.4–2 % for the s wave, 2% for the p wave and 8% for the d wave. Using other analytical forms for the effective potential we were unable to reproduce more closely the experimental p-wave phase shifts without significantly changing the quality of the d-wave phase shifts at the same time. Our calculated phase shifts are of about the same quality (see Fig. 1) as those obtained by Valiron *et al.*[20] with an l-independent model potential (together with orthogonality constraints) subsequently used in NaHe and KHe molecular-structure calculations.[7–9] These authors, however, fitted the experimental phase shifts of Andrick and Bitsch[27] who claim error limits of about 5–20 % depending on the energy.

C. Cross term $V_{\rm CT}(\vec{r}_B,\vec{R})$

In order to have the correct behavior of the adiabatic potential at large internuclear distances, a three-body interaction or cross term has to be included in the calculations.

For large internuclear distance R, and $R>r_A$, the multipole expansion of the interaction between the alkali-metal atom and the rare-gas atom gives, up to the $1/R^6$ order,[20]

$$-\frac{\alpha_{dA}}{2r_A^4}-\frac{\alpha_{qA}-6\beta_A}{2r_A^6}-\frac{\alpha_{dB}r_A^2}{R^6}[1+P_2(\hat{r}_A)]+\frac{3\beta_B}{R^6}\ , \tag{6}$$

where $P_2(\hat{r}_A)$ is a Legendre polynomial. Alternatively, Eq. (6) can be obtained by considering the polarization of B by both the point charges e^- and A,[2,12] and the cross term is then seen to result from the addition of the two electric field vectors produced on B by e^- and A. Then, to be consistent with the cutoff function defined in Eq. (2) the expression of the cross term appears to be

$$V'_{\rm CT}(\vec{r}_B,\vec{R})=-\frac{\alpha_{dB}\xi_B}{(R^2+d_B^2)(r_B^2+d_B^2)}+\frac{1}{2}\frac{\alpha''_{qB}(3\xi_B^2-1)}{(R^2+d_B^2)^{3/2}(r_B^2+d_B^2)^{3/2}}\ , \tag{7}$$

where $\alpha''_{qB}=\alpha_{qB}+2\alpha_{dB}d_B^2$, and $\xi_B=\hat{r}_B\cdot\hat{R}$.

This expression is defined for any value of R and r_B. It is only correct for large values of R, that is, when the electronic charge densities of the two atoms do not overlap and the asymptotic expression (6) can be obtained. For small values of R, the cross term $V'_{\rm CT}(\vec{r}_B,\vec{R})$ depends obviously on the choice of the cutoff function. The situation is different from the case of an isolated atom where the choice of the cutoff is not critical since the determination of the parameters of the short-range interaction [see Eq. (2)] balances any other choice of the cutoff function. Therefore, in the case of the molecular problem, we have defined the cross term as

$$V_{\rm CT}(\vec{r}_B,\vec{R})=V'_{\rm CT}(\vec{r}_B,\vec{R})f_c\left[\frac{R}{r_A}\right]\ , \tag{8}$$

where $f_c(R/r_A)$ is a cutoff function defined as

$$f_c\left[\frac{R}{r_A}\right]=\begin{cases}1-\exp\left[-\left[\dfrac{R}{r_A}-1\right]^2\right] & \text{for } R\geq r_A \quad (9a)\\ 0 \text{ for } R<r_A\ . & (9b)\end{cases}$$

This cutoff function, even though somewhat arbitrary in its analytic form, has to be included in the calculations; it avoids spurious effects which may arise at short internuclear distances. Physically, it is consistent with the fact that the A/R^6 asymptotic form of an adiabatic potential curve will be reached more or less rapidly depending on the degree of excitation of its corresponding alkali-metal atom level. We checked that a more abrupt switching of the cross term does not affect the molecular energies.

D. Core-core interaction $V_{AB}(R)$

We have defined the potential $V_{AB}(R)$ which simulates the alkali-metal-ion–rare-gas-atom interaction as

$$V_{AB}(R)=V_{AB}^{\rm sr}(R)-\frac{1}{2}\frac{\alpha_{dB}}{(R^2+d_B^2)^2}-\frac{1}{2}\frac{\alpha''_{qB}}{(R^2+d_B^2)^3}\ , \tag{10}$$

where $V_{AB}^{\rm sr}(R)$ is a repulsive short-range potential of the form

$$V_{AB}^{\rm sr}(R)=a\exp(-bR)\ . \tag{11}$$

In Eq. (10), the parameters α_{dB}, α''_{qB}, and d are those already determined for He. The parameters a and b for the short-range part of the potential were obtained by fitting the repulsive part of the $X\,^1\Sigma^+$ ground-state potential of

TABLE I. Parameters a and b (in a.u.) for the calculation of the short-range part of the alkali-metal-ion—He $X\,^1\Sigma^+$ potentials.

Alkali-metal ion	Li^+	Na^+	K^+	Rb^+	Cs^+
a	16.0149	52.6812	39.2390	38.2821	49.1559
b	2.4402	2.4884	2.1313	1.8977	1.8747

the alkali-metal-ion—He system determined experimentally or from *ab initio* calculations. Other than for Na^+He, we have chosen to fit the data of Inouye *et al.*[28] who determined repulsive potentials for all the alkali-metal-ion—He systems from experimental values of integral elastic scattering cross sections of the ions in the 0.5—4-keV energy range. In the case of Na^+He, which was the system that we first studied, we have chosen to fit the repulsive part of the *ab initio* calculated potential of Krauss *et al.*,[3] as did Hanssen *et al.*[7] in their model potential calculations; however, the values obtained for the depth D_e of the $X\,^1\Sigma^+$ potential well and for its position R_e are in very close agreement with those obtained when the experimental data of Kita *et al.*[28(b)] are fitted.

The values that we have determined for a and b are reported in Table I. The characteristic parameters D_e, R_e, and R_0 defined as $V(R_0)=0$ that we have obtained for the alkali-metal-ion—He $X\,^1\Sigma^+$ potentials are reported in Table II along with other theoretical[29–31] or experimental results.[32,33] Comparison with experimental data are only possible for the Li^+He $X\,^1\Sigma^+$ potential; we have an overall agreement with the experimental curves as seen in Fig. 2, while the well depths differ by about 20%. The comparisons in Table II indicate that the maximum error for the well depths should be less than 150 cm^{-1} for Li^+He and probably decreases to less than about 5 cm^{-1} for Cs^+He. For Rb^+He and possibly K^+He, the values of the well depths obtained from the scaled electron model of Waldman and Gordon[30] seem to be overestimated.

In the present calculations, we have adopted a quite general method to determine the $X\,^1\Sigma^+$ potential curves of the alkali-metal-ion—He systems, which could be extended to alkali-metal—other-rare-gas-atom systems. This gives the same degree of reliability for our calculations on all M-He systems. However, the comparisons of Table II seem to indicate that the experimental determinations[32,33] of the full $X\,^1\Sigma^+$ potential curve of Li^+He could be more accurate than the one we have used in the molecular-structure calculations of LiHe. The adjustments could be done afterwards case by case since the core-core interaction appears as an additive parameter, for each value of R, in the calculations of the adiabatic potentials.

TABLE II. Characteristic parameters (in a.u.) for the alkali-metal-ion—He $X\,^1\Sigma^+$ potentials: depth (D_e) and position (R_e) of the well potential; R_0 is defined as $V(R_0)=0$.

Alkali-metal ion		Theoretical					Experimental	
		Present	a	b	c	d	e	f
Li^+	D_e	2.094(−3)[g]	2.40(−3)	2.74(−3)	2.573(−3)	1.661(−3)	2.605(−3) ±8%	2.716(−3) ±5%
	R_e	3.75	3.68	3.63	3.65	4.01	3.71 ±2%	3.71
	R_0	3.10	3.05	3.02	3.06	3.50	3.08 ±1%	3.04
Na^+	D_e	1.081(−3)	1.10(−3)		1.286(−3)	9.078(−4)		
	R_e	4.57	4.63		4.575	4.80		
	R_0	3.90	3.90		3.93	4.10		
K^+	D_e	4.786(−4)			8.122(−4)	4.079(−4)		
	R_e	5.62			5.444	5.90		
	R_0	4.80			4.745	2.20		
Rb^+	D_e	2.397(−4)			7.534(−4)	2.720(−4)		
	R_e	6.71			5.73	6.60		
	R_0	5.80			5.01	5.80		
Cs^+	D_e	1.991(−4)				1.801(−4)		
	R_e	7.06				7.41		
	R_0	6.10				6.50		

[a] *ab initio* SCF calculations of Krauss *et al.*(Ref. 3).
[b] *ab initio* calculations (including electron correlations) of Hariharan and Staemmler (Ref. 29).
[c] Scaled electron-gas model of Waldman and Gordon (Ref. 30).
[d] Asymptotic model of Efremenkova *et al.* (Ref. 31).
[e] Molecular-beam experiments of Polak-Dingels *et al.* (Ref. 32).
[f] Alkali-metal-ion mobility measurements of Gatland *et al.* (Ref. 33).
[g] $2.094(-3)=2.094\times10^{-3}$.

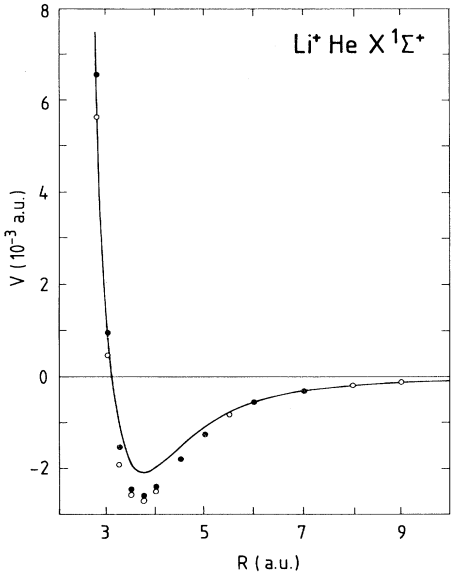

FIG. 2. Potential $V(R)$ for the $X\,^1\Sigma^+$ state of Li^+He. ——, present results [see Eq. (10)]; ●, molecular-beam experimental data of Polak-Dingels *et al.* (Ref. 32); ○, alkali-metal-ion mobility measurements of Gatland *et al.* (Ref. 33).

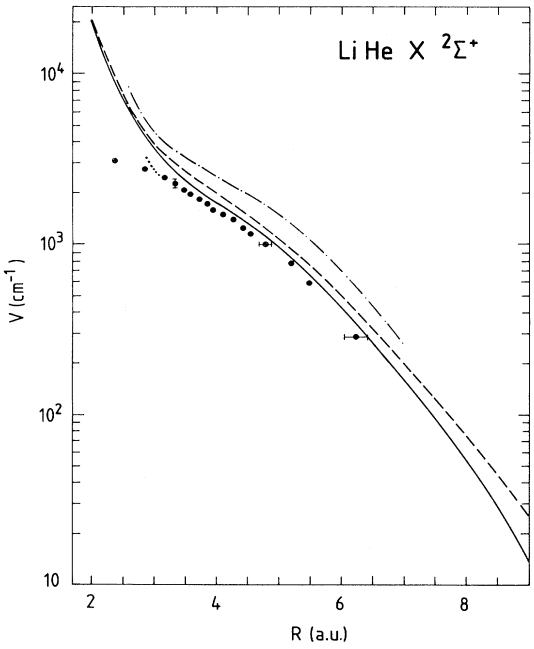

FIG. 3. Potential $V(R)$ for the $X\,^2\Sigma^+$ state of LiHe. ——, present results; — — —, *ab initio* calculations of Krauss *et al.* (Ref. 3); —·—·—·, model potential calculations of Roberts (unpublished, from Ref. 18); ● and · · · ·, experimental data of Havey (Ref. 18).

E. Molecular-structure calculations

The molecular code developed by Junker has been adapted to calculate the interaction energies $E_i(R)$. The molecular wave function $\psi_i(\vec{r}_A,R)$ was expanded over a large basis set of STO for the alkali-metal atom. The internuclear axis $\vec{R}$, which is a symmetry axis for the system, is chosen as the quantization axis. Recalling that the spin-orbit interaction is not included in the present calculations, the projection M_L of the total orbital momentum $\vec{L}$ (in this case, the orbital momentum $\vec{l}$ of the valence electron) along the $\vec{R}$ axis is a good quantum number of the molecular wave function $\psi_i(\vec{r}_A,R)$. Therefore the interaction energies $E_i(R)$ for different values of M_L are obtained from different diagonalizations of the one-electron Hamiltonian. To obtain the $^2\Sigma^+$ states, the STO basis set includes nine STO in order to describe the four lowest nS alkali-metal states, six STO for the three lowest nP states, six STO for the three lowest nD states, four STO for the two lowest nF states, and two STO for the lowest nG states. For the $^2\Pi$ states, a total of 18 STO was used (in fact, 2×18 because $m_l=\pm1$), the parameters of the STO being the same as those for the $^2\Sigma^+$ states. For the $^2\Delta$ states, a total of 12 STO was used, etc. The nonlinear parameters of the STO were optimized at $R=\infty$ and then kept constant for all R values. The large basis set of STO that we have used ensures the stability of the adiabatic potential curves.

III. RESULTS AND DISCUSSIONS

Calculations were performed on all the M-He systems for internuclear distances between 2 and 50 a.u. For obvious reasons, only extracts of our calculations can be reported in this article. However, tabulated interaction energies will be available upon request from the author.

The accuracy of the adiabatic potential curves can only be checked by references to experimental data. Therefore, in the following sections, we want to show for each M-He system that a satisfactory overall agreement has been achieved between our calculations and available experimental data.

A. LiHe system

Figure 3 shows comparisons of our results for the $X\,^2\Sigma^+$ ground state of LiHe with the experimental data of Havey.[18] In this experiment, the potential curves for the $X\,^2\Sigma^+$ and $A\,^2\Pi$ states were obtained from the analysis of the temperature dependence of the far-wing intensities of the LiHe resonance lines; the radial scale factor which has generally to be fixed in this type of experiment[13] was determined absolutely by an independent measurement of the equilibrium position of the $A\,^2\Pi$ potential well.[16] Hence the present comparisons are meaningful. Our $X\,^2\Sigma^+$ potential curve is seen to be in good agreement with the experimental one, while a little more repulsive than the experimental curve; it is, however, less repulsive than the curve obtained from the *ab initio* calculations of Krauss *et al.*[3] and much less repulsive than the one obtained by Roberts (unpublished, from Ref. 18) from model potential calculations.

Using the quasistatic model[13,15] we have calculated, for different experimental temperatures, the normalized red-wing emission spectra corresponding to the $A\,^2\Pi$-$X\,^2\Sigma^+$ transition from

TABLE III. Matrix elements of the dipole moment (in electron bohrs) for the $X\,^2\Sigma^+$-$A\,^2\Pi$ and $X\,^2\Sigma^+$-$B\,^2\Sigma^+$ transitions in LiHe and NaHe.

	LiHe		NaHe	
R	$X\,^2\Sigma^+$-$A\,^2\Pi$	$X\,^2\Sigma^+$-$B\,^2\Sigma^+$	$X\,^2\Sigma^+$-$A\,^2\Pi$	$X\,^2\Sigma^+$-$B\,^2\Sigma^+$
2	2.259	1.614	2.690	2.009
3	2.324	1.646	2.644	1.875
4	2.374	1.991	2.613	2.035
5	2.388	2.133	2.580	2.214
6	2.381	2.201	2.558	2.323
7	2.373	2.257	2.544	2.400
8	2.368	2.300	2.538	2.457
10	2.364	2.348	2.535	2.517
12	2.364	2.361	2.535	2.534
∞	2.364	2.364	2.535	2.535

$$I(\lambda,T)\cong 4\pi g R_\lambda^2 D^2(R_\lambda)\left[\frac{\lambda_0}{\lambda}\right]^4\left|\frac{d}{dR}\Delta V(R)\right|^{-1}_{R=R_\lambda} \times\exp\left[-\frac{V(R_\lambda)}{kT}\right], \tag{12}$$

where g is the statistical weight, R_λ is the internuclear distance associated with emission at the wavelength λ, λ_0 is the wavelength at $R=\infty$, $\Delta V(R)$ is the energy difference between the upper and the lower adiabatic potential curves, $V(R)$ is the adiabatic potential of the upper state relative to its asymptotic value, and $D(R)$ is the matrix element of the dipole moment for the transition. Our calculated values of $D(R)$ for the $X\,^2\Sigma^+$-$A\,^2\Pi$ and $X\,^2\Sigma^+$-$B\,^2\Sigma^+$ transitions in LiHe and NaHe are given in Table III.

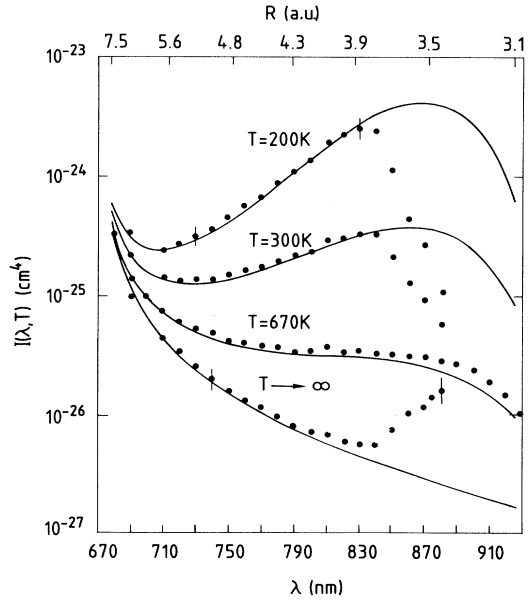

FIG. 4. Temperature dependence of the normalized red-wing emission spectrum of the Li $2P$ state in the presence of He. ●, experimental data of Havey (Ref. 18) (the spectrum at $T=670$ K is that of Scheps *et al.* [Ref. 13(d)]); ——, present results normalized at $\lambda=700$ nm on the $T=670$ K spectrum. Spectra are also reported vs the internuclear distance R at which the light emission occurs.

The calculated emission spectra for the LiHe are shown in Fig. 4 along with the experimental ones.[18] The experimental emission spectrum at $T=670$ K is that measured by Scheps *et al.*,[13(d)] while the ones at other temperatures are an extension by Havey[18] of these data obtained from an experimental temperature dependence of the red wing.[17] Our calculated spectrum at $T=670$ K is in excellent agreement with the experimental one over the entire wavelength range. The calculated spectra for the other temperatures are also in excellent agreement with the experimental ones up to $\lambda\cong 830$ nm, but differ drastically afterwards. The reason given by Havey to explain the sudden increase of the T_∞ spectra for $\lambda>830$ nm is that the matrix dipole moment should increase strongly. This is in contradiction with the present results (see Table III) and those of Krauss *et al.*[3] A possible explanation is that an experimental problem may have arisen in the detection of the emission light for $\lambda>830$ nm. It is worthwhile noting that the discrepancies between our calculated spectra and the experimental ones of Havey occur at $R\lesssim 3.9$ a.u. This explains the differences between the characteristics of our $A\,^2\Pi$ potential ($D_e=1025$ cm^{-1} at $R_e=3.44$ a.u.) and those of the experimental one ($D_e=850\pm100$ cm^{-1} at $R_e=3.45\pm0.08$ a.u.). The *ab initio* values of Krauss *et al.*[3] are $D_e=500$ cm^{-1} at $R=3.5$ a.u., while unpublished model potential calculations of Roberts (see Ref. 18) give $D_e=850$ cm^{-1} at $R_e=3.5$ a.u. Our blue-wing emission spectrum for the $B\,^2\Sigma^+$-$X\,^2\Sigma^+$ transition, not reported in Fig. 4, is also in excellent agreement with the data of Scheps *et al.*,[13(d)] indicating that our $B\,^2\Sigma^+$ potential curve is probably well predicted.

This agreement between our spectra and those measured by Hedges *et al.* or those experimentally determined by Havey up to $\lambda=830$ nm, is not altered when using the $X\,^1\Sigma^+$ potential of Li^+He obtained from the molecular-beam experiment of Polak-Dingels *et al.*[32] in the molecular-structure calculations of LiHe.

In summary, our adiabatic potentials for LiHe seem to be in better overall agreement with experimental data than are other calculations.

B. NaHe

The present calculations can explain the long-wavelength discrepancy between the red-wing spectrum of the $3\,^2P$ resonance line of Na broadened by He measured by York *et al.*[13(c)] at $T=403$ K and that calculated by

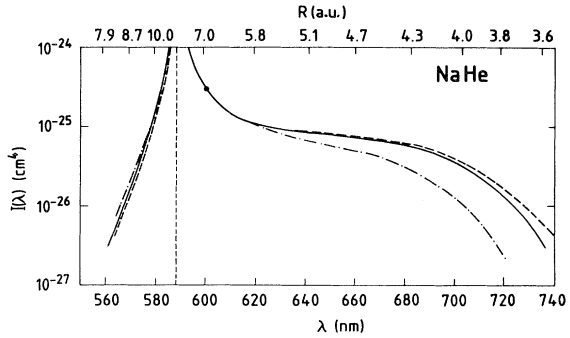

FIG. 5. Normalized emission spectra of the Na $3P$ state in the presence of He at $T=403$ K. Dashed line, experimental data of York *et al.* [Ref. 13(c)]; ——, present results; —·—·—·, results of Hanssen *et al.* (Ref. 7). Calculated spectra have been normalized to the experimental one at $\lambda=600$ nm. As in Fig. 4, the spectra are also reported vs the internuclear distance R at which the light emission occurs.

Hanssen *et al.*[7] from their model potential. These authors concluded in their article that the discrepancy could not be explained by uncertainties in the calculated interaction potentials.

We have calculated the blue- and red-wing spectra with our potentials from Eq. (12). They are shown in Fig. 5 along with those calculated by Hanssen *et al.* and those measured by York *et al.* Our calculated spectra are in very good agreement with the experimental data over the entire wavelength range. Since the ground-state potential curve of Hanssen *et al.* is in good agreement with ours (see Fig. 6), the differences observed in the red-wing spectra are due to different $^2\Pi\,3P$ potential curves. Our $^2\Pi\,3P$ potential curve is the most attractive. Indeed, at $R=4.0$ a.u., the difference in the potential wells is $\Delta V\cong 220$ cm^{-1} corresponding to an increase in the intensity of our spectrum relative to that of Hanssen by $\exp(\Delta V/kT)\cong 2.2$ at $T=403$ K. This in agreement with what it is observed in Fig. 5, noting that for $R=4.0$ a.u. the corresponding wavelength obtained by Hanssen *et al.* is about 697 nm in comparison with our value of 704 nm. These conclusions are confirmed by recent measurements of Havey *et al.*[15] who found a well depth $D_e=480\pm 50$ cm^{-1} at $R_e=4.4\pm 0.2$ a.u., in much better agreement with our results, $D_e=511$ cm^{-1} at $R_e=4.35$ a.u., than with the results of Hanssen *et al.*, $D_e=299$ cm^{-1} at $R_e=4.58$ a.u. As expected, our results are also consistent with the temperature-dependence measurements of Havey *et al.*[15] for the red-wing spectrum.

Finally, Fig. 5 also shows that our calculated blue-wing spectrum agrees more closely with the measured spectrum than that calculated by Hanssen *et al.*; this is consistent with the fact that the $^2\Sigma^+\,3P$ potential curve of Hanssen *et al.* is more attractive than ours (see Fig. 6).

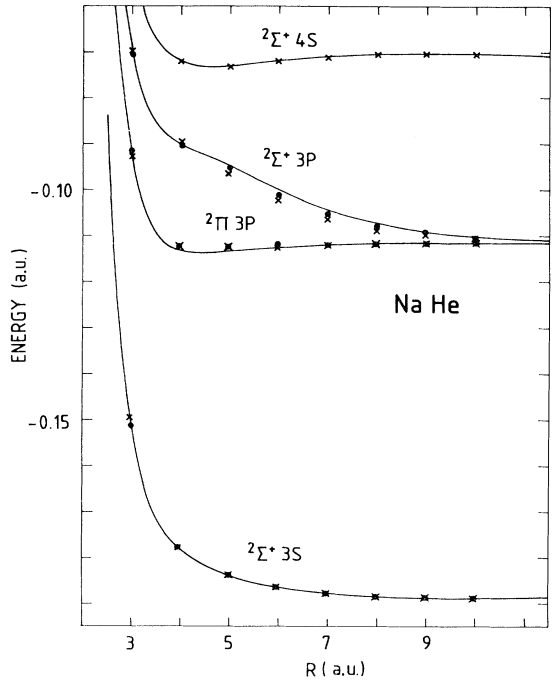

FIG. 6. Energies of the lowest states of the NaHe system. ——, present results; ×, model potential calculations of Hanssen *et al.* (Ref. 7); ●, *ab initio* calculations of Krauss *et al.* (Ref. 3). Arrows indicate the position of the asymptotic energies.

C. KHe

For KHe, no measurements have been made of the far-wing intensities of the resonance lines of K broadened by He. However, there is a very accurate measurement of the energy dependence of the cross section for the $4^2P_{1/2}\rightarrow 4^2P_{3/2}$ transition in K induced in collisions with He in the 0.06—0.35-eV energy range obtained from a cross-beam experiment.[34] The measured cross sections were normalized to the recent absolute value of the cross

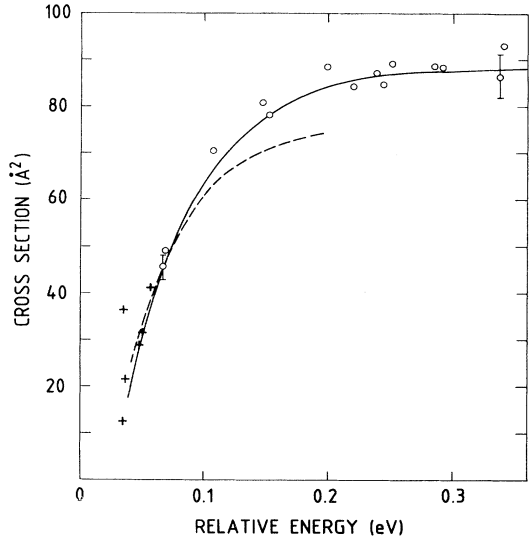

FIG. 7. Energy dependence of the cross section for the $4^2P_{1/2}\rightarrow 4^2P_{3/2}$ transition in K induced in collisions with He. ○, cross-beam experimental data of Mestdagh *et al.* (Ref. 34) normalized on the cell-experimental data of Boggy and Franz (Ref. 35); ×, cross-beam experimental data of Anderson *et al.* (Ref. 36); ——, present results; — — —, theoretical results of Masnou-Seeuws (Ref. 9).

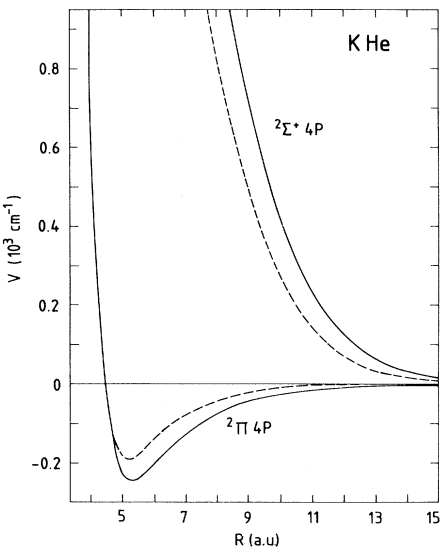

FIG. 8. $^2\Pi$ 4P and $^2\Sigma^+$ 4P potential curves of KHe. ——, present results; — — —, model potential calculations of Masnou-Seeuws (Ref. 9).

section determined by Boggy and Franz[35] from a cell-type experiment at $T=380$ K, so that direct comparisons with theoretical calculations are now possible. In Fig. 7, cross-beam experimental data are shown along with our calculations and those of Masnou-Seeuws[9] obtained using adiabatic potentials determined from recent model potential calculations. Note that the theoretical cross sections are obtained from exact quantum-mechanical calculations.[37] Our results are seen to be within the experimental uncertainties, while the energy dependence of the cross sections

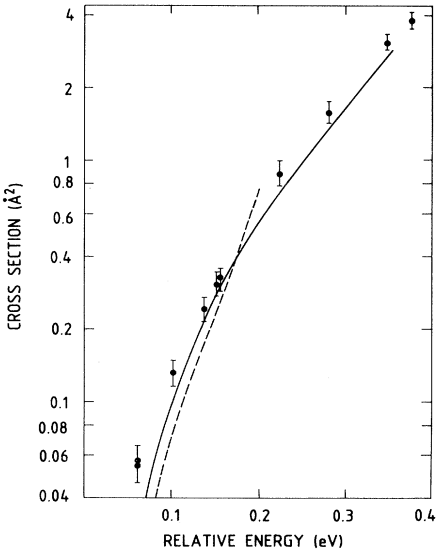

FIG. 9. Energy dependence of the cross section for the $5^2P_{1/2} \rightarrow 5^2P_{3/2}$ transition in Rb induced by collisions with He. ●, cross-beam experimental data of Mestdagh *et al.* (Ref. 34) normalized on the cell-experimental data of Gallagher (Ref. 38); ——, present results; — — —, results of Olson (Ref. 39) using the adiabatic potentials of Baylis (Ref. 2).

obtained by the calculations of Masnou-Seeuws is too weak. It is well known (see, for example, Nikitin[1]) that the fine-structure cross sections are mainly determined by the difference $\Delta V(R)$ between the potential curves of the $A\,^2\Pi$ and $B\,^2\Sigma^+$ states. In particular, the maximum of the cross section is mainly sensitive to a radial coupling localized at an internuclear distance R_0 such that $\Delta V(R_0)=\Delta\epsilon$ ($\Delta\epsilon$ is the energy splitting of the ^2P_j levels); a rotational coupling localized at short internuclear distances, where the $A\,^2\Pi_{1/2}$ and $A\,^2\Pi_{3/2}$ potential curves are nearly parallel and repulsive, may also contribute significantly to the values of the cross sections. In the present case, $R_0 \cong 12.5$ a.u., where the $A\,^2\Pi$ potential curve is nearly zero. Therefore the experimental data check mainly the repulsivity of the $^2\Sigma^+$ 4P potential curve. The more repulsive the $^2\Sigma^+$ 4P potential curve, the larger is the maximum of the cross section. The results in Fig. 7 are consistent with the differences observed in Fig. 8 between the calculated potential curves. Our $^2\Sigma^+$ 4P potential curve is seen to be more repulsive and our $^2\Pi$ 4P potential curve more attractive than those obtained by Masnou-Seeuws. It is worthwhile noting that the same differences occur between our results and those of Masnou-Seeuws for KHe, and between our results and those of Hanssen *et al.*[7] for NaHe; this is consistent with the fact that both the molecular-structure calculations used the same l-independent model potential together with orthogonality constraints.

D. RbHe

In the case of RbHe, no attempt was made by Drummond and Gallagher[13(b)] to determine the adiabatic potential associated with the $5^2P_{1/2}$ and $5^2P_{3/2}$ states of a Rb atom from the far-wing intensity measurements of the resonance lines in the presence of a He atom. While our calculated spectra, after having included the spin-orbit interaction as a perturbation[37] to obtain the adiabatic potentials associated with the $5^2P_{1/2}$ and $5^2P_{3/2}$ states of Rb, are consistent with those measured by the above authors, more experimental and theoretical work seems to be desirable for meaningful comparisons.

As for KHe, we can test our calculated potentials by comparisons with the cross-beam energy-dependence measurements[34] of the cross section for the $5^2P_{1/2} \rightarrow 5^2P_{3/2}$ transition in Rb induced in collisions with He in the 0.06—0.20-eV energy range. For the same fine-structure transition, Gallagher[38] studied in a cell experiment the temperature dependence of the cross section averaged over a Maxwell-Boltzmann distribution of velocities, and derived afterwards the energy dependence of the nonaveraged cross section. His data are in excellent agreement with those of the cross-beam experiment[34] in the 0.13—0.40-eV energy range so that the latter were normalized at $E=0.15$ eV to Gallagher's result. In Fig. 9 our results are shown along with the cross-beam experimental data and the theoretical results obtained by Olson[39] using the adiabatic potentials of Baylis.[2] Our results are in good agreement with experimental results in the 0.1—0.4-eV energy range. The energy dependence of the cross section is well predicted while the differences observed in the absolute values, less than 20%, may be due to the choice of normalization energy. For $E<0.1$ eV our cross sections are smaller than the experimental ones, but because the

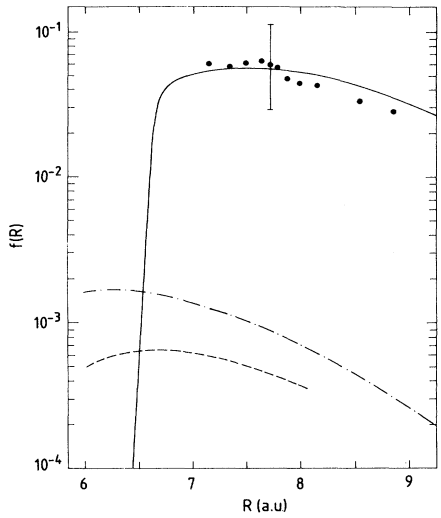

FIG. 10. Dipole-induced oscillator strength vs the internuclear distance R for the $^2\Sigma^+ 6S$-$^2\Sigma^+ 5D$ transition in CsHe. ——, present results; —·—·—·, l-independent pseudopotential calculations of Pascale (Ref. 40); — — —, l-independent pseudopotential calculations of Czuchaj (Ref. 41); ●, absolute experimental data of Ferray *et al.* (Ref. 14).

cross sections are relatively small (less than 10^{-17} cm^2) the experimental uncertainties may be larger than estimated.

In contrast, the energy dependence of the cross section obtained by Olson is seen to be much too strong. Therefore the overall agreement obtained between our calculations and the cross-beam data for the $5^2P_{1/2} \rightarrow 5^2P_{3/2}$ transition cross section indicates that the repulsive strength of the $^2\Sigma^+ 5P$ potential curve is correctly calculated, and it is expected that the same degree of accuracy has been obtained for the other potential curves.

E. CsHe

We have already shown[21] the very good agreement that we have obtained with the experimental data of Ferray *et al.*[14] for the $^2\Sigma^+ 5D$ potential curve of CsHe. This agreement is confirmed by the calculation of the oscillator strength for the $^2\Sigma^+ 6S$-$^2\Sigma^+ 5D$ transition. The results are shown in Fig. 10. Our results are in excellent agreement with the experimental data, while previous calculations of the oscillator strength[40,41] are seen about two orders of magnitude lower. The rapid change in the oscillator strength for $R < 7$ a.u. corresponds to the pronounced avoided crossing observed in Fig. 11 between the $^2\Sigma^+ 5D$ and $^2\Sigma^+ 7S$ potential curves. In this region the $^2\Sigma^+ 5D$ and $^2\Sigma^+ 7S$ states exchange their characteristics. Calculations of the spectra associated with the $^2\Sigma^+ 6S$-$^2\Sigma^+ 5D$ and $^2\Sigma^+ 6S$-$^2\Sigma^+ 7S$ are currently in progress. It is worthwhile noting that the avoided crossing between the $^2\Sigma^+ 7P$ and $^2\Sigma^+ 6D$ potential curves observed in Fig. 11 is probably responsible for the large cross section measured by Cuvellier *et al.*[42] for the $7P \rightarrow 6D$ transition, which could not be explained by the structureless adiabatic potential curves obtained from l-independent pseudopotential calculations.[6]

Finally, our results for the $A\,^2\Pi_{3/2}$ and the $A\,^2\Pi_{1/2}$ states (after having included the spin-orbit interaction as a perturbation) are consistent with the pioneering measurements of Hedges *et al.*[13(a)] who estimated a well depth $D_e \cong 170$ cm^{-1} at $R_e \cong 7.65$ a.u. for the $A\,^2\Pi_{3/2}$ state and found a mainly repulsive $A\,^2\Pi_{1/2}$ potential curve. For the $A\,^2\Pi_{3/2}$ state, we have found $D_e = 114$ cm^{-1} at $R_e = 6.70$ a.u., while the $A\,^2\Pi_{1/2}$ potential curve presents a "suspended well" ($D_e = 60$ cm^{-1} at $R_e = 6.70$ a.u.) and a potential barrier of about 80 cm^{-1} at $R \cong 9.5$ a.u.; that is within the experimental uncertainties. However, the shape of our

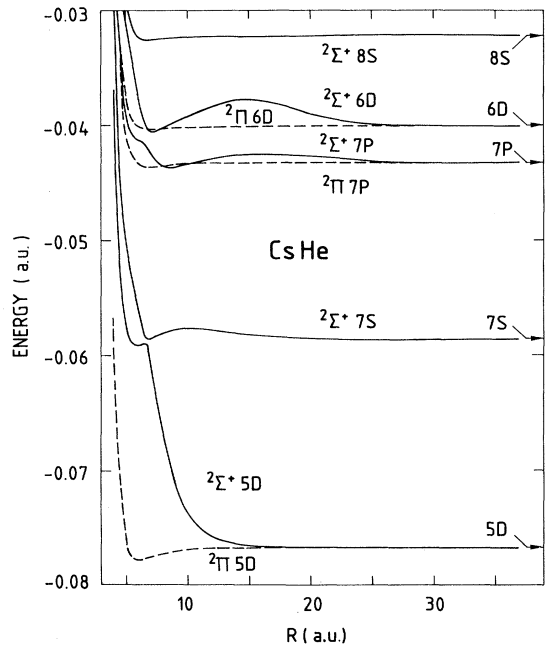

FIG. 11. Energies of some excited states of CsHe. Present results: ——, $^2\Sigma^+$ states; — — —, $^2\Pi$ states. Arrows indicate the position of the asymptotic energies.

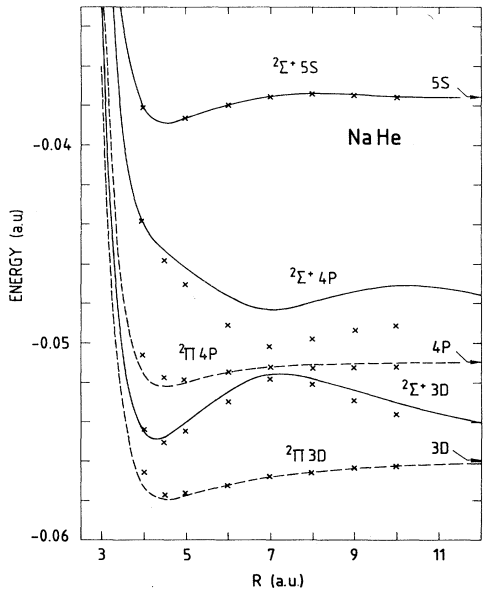

FIG. 12. Energies of some excited states of NaHe, as in Fig. 11. ×'s are the model potential calculations of Hanssen *et al.* (Ref. 7).

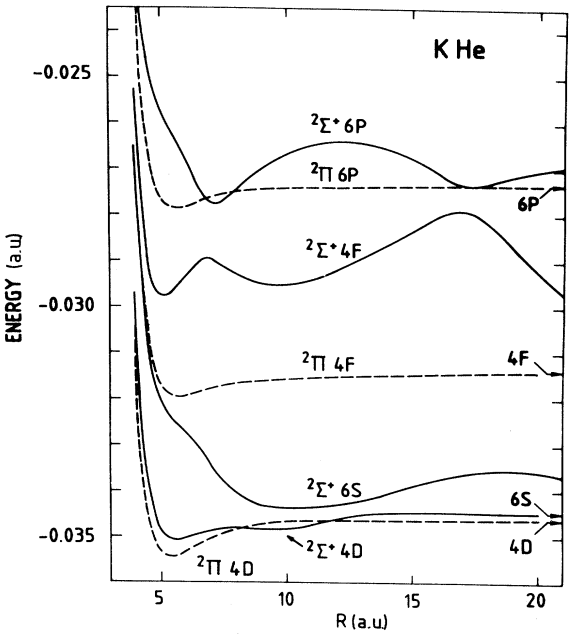

FIG. 13. Energies of some excited states of KHe, as in Fig. 11.

$B\,^2\Sigma^+_{1/2}$ potential curve, which presents a structure, is different from the monotonic repulsive curve assumed by Hedges *et al.* to analyze their data.

F. General considerations

The overall agreement that we obtained for all the M-He systems between our results and experimental data indicates that significant improvements have been achieved in the calculations of the adiabatic potential curves by using an l-dependent pseudopotential technique.

In Figs. 12–14 we have shown as examples some potential-energy curves for excited states of NaHe, KHe, and RbHe systems. In general, in contrast with the structureless potential curves obtained previously from l-independent pseudopotential caculations,[6–10] the present potential curves exhibit several avoided crossings, indicating that some electronic transitions or quenching processes are probably efficient in thermal or suprathermal collisions of excited alkali-metal atoms with He atoms.

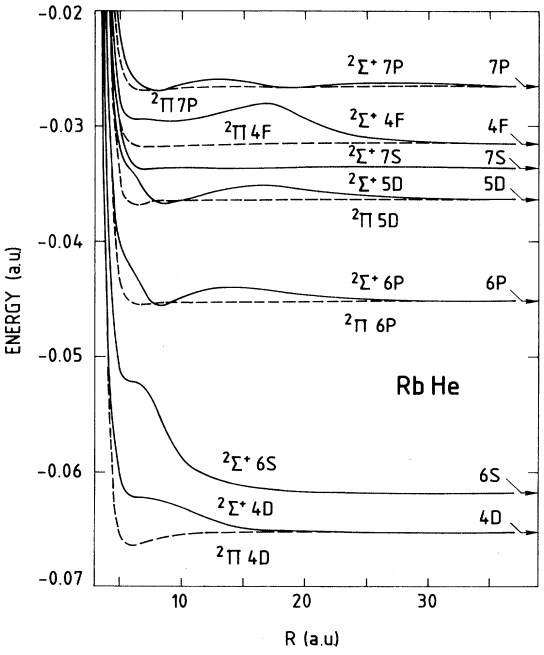

FIG. 14. Energies of some excited states of RbHe, as in Fig. 11.

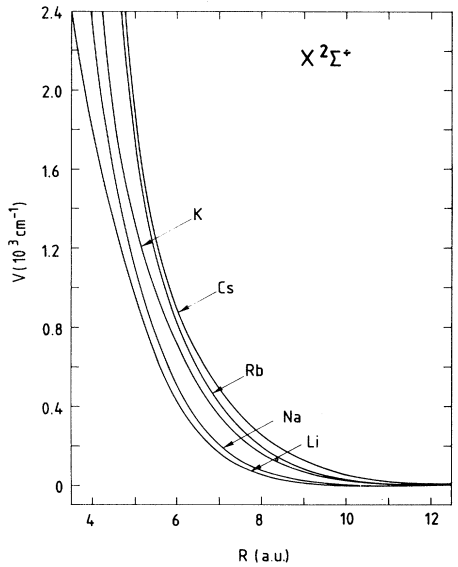

FIG. 15. Potentials $V(R)$ for the $X\,^2\Sigma^+$ states of the M-He systems.

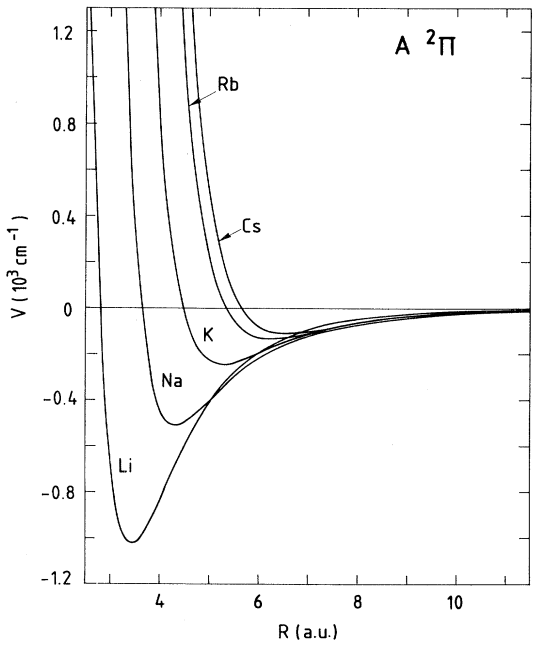

FIG. 16. Potentials $V(R)$ for the $A\,^2\Pi$ states of the M-He systems.

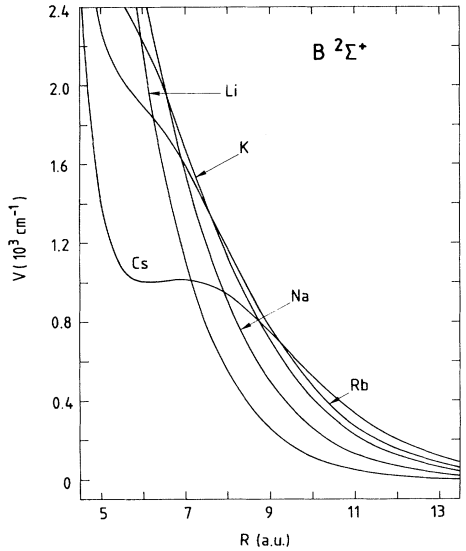

FIG. 17. Potentials $V(R)$ for the $B\,^2\Sigma^+$ states of the M-He systems.

Comparisons with the model potential calculations of Hanssen *et al.*[7] for NaHe are shown in Fig. 12; it is seen that while the two calculations agree roughly, our $^2\Sigma^+$ $4P$ potential curve is much more repulsive than that found by these authors and does not exhibit the pronounced avoided crossing with the $^2\Sigma^+$ $3D$ potential curve they obtained. It should be noted that our $^2\Sigma^+$ $4P$ potential curve reaches its asymptote for $R > 25$ a.u.

In Figs. 15–17 the adiabatic potential curves for the $X\,^2\Sigma^+$, $A\,^2\Pi$, and $B\,^2\Sigma^+$ states are presented for all the M-He systems. This allows us to discuss the characteristics of these curves when one goes from Li to Cs. It is observed that the repulsive strength of the same potential curve increases from Li to Cs. This is due to a more tightened wave function in the case of the lightest alkali-metal atoms which therefore can approach more closely the He atom. For the $B\,^2\Sigma^+$ states, however, coupling with upper states (mainly with the immediate upper state) increases from Li to Cs because of decreasing asymptotic energy separations between the $n\,^2P$ levels and their neighboring upper levels. This results in a structure more or less pronounced in the $B\,^2\Sigma^+$ potential curve and a change in the order of their repulsive strengths at small internuclear distances. Very shallow potential wells (from $D_e = 2.5$ cm^{-1} at $R_e = 11.4$ a.u. in the case of LiHe to $D_e = 1.3$ cm^{-1} at $R_e = 15.0$ a.u. in the case of CsHe) are found for the $X\,^2\Sigma^+$ ground states, in agreement with previous calculations.[2,6,43] The potential wells for the $B\,^2\Sigma^+$ states are found shallower (< 1 cm^{-1}) than those for the $X\,^2\Sigma^+$ states and located at larger internuclear distances (~ 18–23 a.u.). The well depths for the $A\,^2\Pi$ states increase when one goes from Cs to Li (see Fig. 16). They are found considerably deeper than those of our previous calculation[6] which used an l-independent pseudopotential to represent the interaction between the valence electron and the He atom. Contrary to the $B\,^2\Sigma^+$ state, the $A\,^2\Pi$ state cannot have any s-wave character. Therefore, because there are only two s orbitals in the He core and an l-dependent pseudopotential has been used to describe the e^--He interaction, the He atom can approach the alkali-metal atom more closely for the $A\,^2\Pi$ state than it can when using an l-independent pseudopotential. Finally, for the same M-He system, the fact that the $B\,^2\Sigma^+$ potential curve is the most repulsive, and the $A\,^2\Pi$ potential curve the most attractive, is well understood in terms of electronic distribution.[2,3]

Table IV summarizes the well depths obtained for the $A\,^2\Pi$ states with comparisons with previous determinations. As previously discussed, our results are in good agreement with recent experimental data for LiHe[18] and NaHe.[15] Our well depths are much larger than those obtained from *ab initio* calculations[3] or from model potential calculations with orthogonality constraints[7,9]; they are in much closer agreement with recent unpublished model po-

TABLE IV. Depth (D_e in cm^{-1}) and position (R_e in a.u.) of the $A\,^2\Pi$ potential wells of the M-He systems.

Alkali-metal		Li	Na	K	Rb	Cs
Present	D_e	1025	511	245	134	112
	R_e	3.44	4.35	5.30	6.25	6.60
a	D_e	500	210			
	R_e	3.5	4.53			
b	D_e		299	190		
	R_e		4.58	5.30		
c	D_e	850	427			
	R_e	3.5	4.27			
d	D_e	850±100	480±50			
	R_e	3.45±0.08	4.4±0.2			

[a] *ab initio* SCF calculations of Krauss *et al.* (Ref. 3).
[b] Model potential calculations of Hanssen *et al.* (Ref. 7) for NaHe and of Masnou-Seeuws for KHe.
[c] Model potential calculations of Roberts (unpublished) for LiHe (taken from Ref. 18) and of Peach (unpublished) for NaHe (taken from Ref. 44).
[d] Experimental results of Havey (Ref. 18) for LiHe and Havey *et al.* (Ref. 15) for NaHe.

tential calculations (from Refs. 18 and 44). Despite the suggestions in Refs. 8, 9, and 20 that only model potentials with explicit orthogonality constraints be used for He and Ne, it is worthwhile to stress that pseudopotentials work very well if they are l dependent, as is demonstrated by the present results.

IV. CONCLUSIONS

Using an l-dependent pseudopotential technique we have made extensive molecular-structure calculations for all the M-He systems from the ground state up to highly excited states. In view of the satisfactory overall agreement with all available experimental data, we believe our calculations are quite accurate, in spite of somewhat arbitrary but unavoidable choice in the cutoff functions used[45] or in the alkali-metal-ion—He interaction. In general, our calculations agree much more closely with the experimental data than all previously published calculations, indicating that a large improvement in the calculation of the adiabatic potential curves for all the alkali-metal—He systems has been achieved by using the l-dependent pseudopotential technique. Therefore we hope these calculations will stimulate more experimental work on these systems. Extension of these calculations to alkali-metal—other-rare-gas-atom systems are now in progress.

ACKNOWLEDGMENTS

The author is indebted to Dr. B. R. Junker for providing him with the molecular-structure code. He thanks Professor R. E. Olson, Dr. B. R. Junker, Dr. A. Valance, and Dr. C. Murez for helpful discussions; Dr. J. Berlande, Dr. J. M. Mestdagh, and Dr. B. Sayer for useful comments on the manuscript. He also thanks Dr. A. P. Hickman for the use of his computer program to calculate the phase shifts, and Dr. M. D. Havey for providing him with experimental data on LiHe potentials prior to publication. He is grateful to Dr. C. Manus and J. Berlande for their encouragement and support during the course of this work.

[1]See, for example, E. E. Nikitin, Adv. Chem. Phys. 28, 317 (1975); L. Krause, *ibid.* 28, 267 (1975); W. E. Baylis, in *Progress in Atomic Spectroscopy,* edited by W. Hanle and H. Kleinpoppen (Plenum, New York, 1979), Chap. 6, p. 207 and Chap. 28, p. 1227; M. Elbel, *ibid.,* Chap. 29, p. 1299; W. H. Breckenridge and H. Umemoto, in *Dynamics of Excited State,* edited by K. P. Lawley (Wiley, New York, 1982), p. 325; J. M. Mestdagh, thèse, Université de Paris—Nord, 1982 (unpublished); B. Sayer, Acta Phys. Pol. A 61, 531 (1982).

[2]W. E. Baylis, J. Chem. Phys. 51, 2665 (1969).

[3]M. Krauss, P. Maldonado, and C. Wahl, J. Chem. Phys. 54, 4944 (1971).

[4]R. P. Saxon, R. E. Olson, and B. Liu, J. Chem. Phys. 67, 2692 (1977).

[5]C. Bottcher, Chem. Phys. Lett. 18, 457 (1973).

[6]J. Pascale and J. Vandeplanque, J. Chem. Phys. 60, 2278 (1974).

[7]J. Hanssen, R. McCarroll, and P. Valiron, J. Phys. B 12, 899 (1979).

[8]F. Masnou-Seeuws, M. Philippe, and P. Valiron, Phys. Rev. Lett. 41, 395 (1978).

[9]F. Masnou-Seeuws, J. Phys. B 15, 883 (1982).

[10]E. Czuchaj and J. Sienkiewicz, Z. Naturforsch. A 34, 694 (1979).

[11]R. Düren and G. Moritz, J. Chem. Phys. 73, 5155 (1980).

[12]G. Peach, Comments At. Mol. Phys. 11, 101 (1982).

[13](a) R. E. M. Hedges, D. L. Drummond, and A. Gallagher, Phys. Rev. A 6, 1519 (1972); (b) D. L. Drummond and A. Gallagher, J. Chem. Phys. 60, 3426 (1974); (c) G. York, R. Scheps, and A. Gallagher, *ibid.* 63, 1052 (1975); (d) R. Scheps, Ch. Ottinger, G. York, and A. Gallagher, *ibid.* 63, 2581 (1975).

[14]M. Ferray, J. P. Visticot, J. Lozingot, and B. Sayer, J. Phys. B 13, 2571 (1980); see also references therein.

[15]M. D. Havey, S. E. Frolking, and J. J Wright, Phys. Rev. Lett. 45, 1783 (1980).

[16]M. D. Havey, Phys. Rev. Lett. 48, 1100 (1982).

[17]L. C. Balling, J. J. Wright, and M. D. Havey, Phys. Rev. A 26, 1426 (1982).

[18]M. D. Havey, J. Chem. Phys. (in press).

[19]J. N. Bardsley, Case Stud. At. Phys. 4, 299 (1974).

[20]P. Valiron, R. Gayet, R. McCarroll, F. Masnou-Seeuws, and M. Philippe, J. Phys. B 12, 53 (1979).

[21]J. Pascale, Phys. Rev. A 26, 3709 (1982). We have found an error in the calculation of the three-body interaction term. However, this does not affect significantly the results and conclusions reported.

[22]M. A. Thomas and J. W. Humberston, J. Phys. B 5, L229 (1972).

[23]R. R. Teachout and R. T. Pack, At. Data 3, 195 (1971).

[24]A. Dalgarno, G. W. F. Drake, and G. A. Victor, Phys. Rev. 176, 194 (1968).

[25]J. F. Williams, J. Phys. B 12, 265 (1979).

[26]T. F. O'Malley, P. G. Burke, and K. A. Berrington, J. Phys. B 12, 953 (1979).

[27]D. Andrick and A. Bitsch, J. Phys. B 8, 393 (1975).

[28](a) H. Inouye and S. Kita, J. Phys. Soc. Jpn. 34, 1588 (1973); (b) S. Kita, K. Noda, and H. Inouye, J. Chem. Phys. 63, 4930 (1975); (c) H. Inouye and S. Kita, *ibid.* 56, 4877 (1972); (d) H. Inouye, K. Noda, and S. Kita, *ibid.* 71, 2136 (1979).

[29]P. C. Hariharan and V. Staemmler, Chem. Phys. 15, 409 (1976).

[30]M. Waldman and R. G. Gordon, J. Chem. Phys. 71, 1325 (1979).

[31]L. Ya. Efremenkova, A. A. Radsig, and B. M. Smirnov, Opt. Spekstrosk. 36, 61 (1974) [Opt. Spectrosc. (USSR) 36, 35 (1974)].

[32]P. Polak-Dingels, M. S. Rajan, and E. A. Gislason, J. Chem. Phys. 77, 3983 (1982).

[33]I. R. Gatland, W. F. Morrison, H. W. Ellis, M. G. Thackston, E. W. McDaniel, M. H. Alexander, L. A. Viehland, and E. A. Mason, J. Chem. Phys. 66, 5121 (1977).

[34]J. M. Mestdagh, thèse, Université de Paris—Nord, 1982 (unpublished). See also references therein.

[35]R. Boggy and F. A. Franz, Phys. Rev. A 25, 1887 (1982).

[36]R. W. Anderson, J. P. Goddard, C. Parravano, and J. Warner, J. Chem. Phys. 64, 4037 (1976).

[37]R. H. D. Reid, J. Phys. B 6, 2018 (1973).

[38]A. Gallagher, Phys. Rev. 172, 88 (1968).

[39]R. E. Olson, Chem. Phys. Lett. 33, 250 (1975).

[40]J. Pascale, J. Chem. Phys. 67, 204 (1977).

[41]E. Czuchaj, Z. Phys. A 292, 109 (1979).

[42]J. Cuvellier, P. R. Fournier, F. Gounand, J. Pascale, and J. Berlande, Phys. Rev. A 11, 846 (1975).
[43]G. Das and A. C. Wahl, Phys. Rev. A 4, 825 (1971).
[44]P. Ewart and S. V. O'Leary, J. Phys. B 15, 3669 (1982).
[45]Our calculations are not very sensitive with respect to reasonable variations of the radius cutoff d_B. For example, in the case of NaHe, taking $d_B=0.7$ a.u. in place of 1.0 a.u. changes by about 1% the well depths of the $X\,^2\Sigma^+$ and $A\,^2\Pi$ states; taking $d_B=1.2$ a.u. changes by about 4% the well depth of the $X\,^2\Sigma^+$ state and by about 2% that of the $A\,^2\Pi$ state.